

REPORT DOCUMENTATION PAGE		READ INSTRUCTIONS BEFORE COMPLETING FORM
1. REPORT NUMBER	2. GOVT ACCESSION NO.	3. RECIPIENT'S CATALOG NUMBER
4. TITLE (and Subtitle) Measurement of Sound Propagation, Down Slope to a Bottom Limited Sound Channel		5. TYPE OF REPORT & PERIOD COVERED
		6. PERFORMING ORG. REPORT NUMBER
7. AUTHOR(s) William M. Carey, NORDA, I. Gereben, TRW, B. A. Brunson, PSI, M. R. Bradley, PSI		8. CONTRACT OR GRANT NUMBER(s)
9. PERFORMING ORGANIZATION NAME AND ADDRESS Naval Ocean Research and Development Activity Code 113 NSTL, Mississippi 39529-5004		10. PROGRAM ELEMENT, PROJECT, TASK AREA & WORK UNIT NUMBERS
11. CONTROLLING OFFICE NAME AND ADDRESS Naval Ocean Research and Development Activity Code 113 NSTL, Mississippi 39529-5004		12. REPORT DATE August 1985
		13. NUMBER OF PAGES 42
14. MONITORING AGENCY NAME & ADDRESS (if different from Controlling Office)		15. SECURITY CLASS. (of this report) Unclassified
		15a. DECLASSIFICATION/DOWNGRADING SCHEDULE
16. DISTRIBUTION STATEMENT (of this Report)		
17. DISTRIBUTION STATEMENT (of the abstract entered in Block 20, if different from Report) Distribution Unlimited		
18. SUPPLEMENTARY NOTES		
19. KEY WORDS (Continue on reverse side if necessary and identify by block number) Down-Slope Propagation, Coherence, ASTRAL, FACT, P.E. Transmission, Bottom Loss, Geoacoustic, SNAP, Normal Mode		
20. ABSTRACT (Continue on reverse side if necessary and identify by block number) Signal transmission loss and spatial coherence data for source-receiver separations between 100 and 250 km were acquired in the Gulf of Mexico with a calibrated seismic measurement system (400 m deep), a towed projector (100 m deep) which emitted 67 and 173 Hz tones, and a moored Webb sound source at 988 m depth driven at 175 Hz. Environmental data such as the range dependent bathymetry and sound velocity profiles were measured. The 67 Hz data showed a persistent sound transmission loss of approximately 90 dB whereas the 173 Hz showed several pronounced loss minima between 100-90 dB. Slope enhancements		

were found to be on the order 2-4 dB @ 67 Hz and 6 dB @ 173 Hz when compared to flat bottom calculations. Pair-wise coherence data show the combined effects of multipath interference and signal-to-noise ratio. Estimates of signal coherence length from the coherent summation of streamer hydrophones yield coherence lengths between 70 and 300 meters at a frequency of 173 Hz. Fast asymptotic coherent and normal mode transmission loss calculations produced results consistent with measured data for the deep flat portion of the measurement tracks when measured geo-acoustic profiles or related bottom loss curves were used. The implicit finite difference parabolic equation calculations were consistent with range-averaged data for the flat portion of the track as well as on the slope. These results show that if proper qualitative description of the sub-bottom velocity profiles are used, then computations with either a parabolic equation or normal mode technique are consistent with experimental results.



Measurement of Sound Propagation, Down Slope to a Bottom-Limited Sound Channel

William M. Carey
Code 113
Naval Ocean Research and Development Activity

I. Gereben
TRW

B. A. Brunson
Planning Systems Incorporated

M. R. Bradley
Planning Systems Incorporated

Presented at the 109th Meeting of the Acoustical Society of America,
Paper F7, 8-12 April 1985, Austin, Texas

*Reproduction in whole or in part is permitted
for any purpose of the United States Government.
Document cleared for public release and sale;
distribution unlimited.*

*Naval Ocean Research and Development Activity.
NSTL, Mississippi 39529*

MEASUREMENT OF SOUND PROPAGATION, DOWN SLOPE TO
A BOTTOM-LIMITED SOUND CHANNEL

William M. Carey
Code 113
Naval Ocean Research and Development Activity

I. Gereben
TRW

B. A. Brunson
Planning Systems Incorporated

M. R. Bradley
Planning Systems Incorporated

Presented at the 109th Meeting of the Acoustical Society
of America, Paper F7, 8-12 April 1985, Austin, Texas

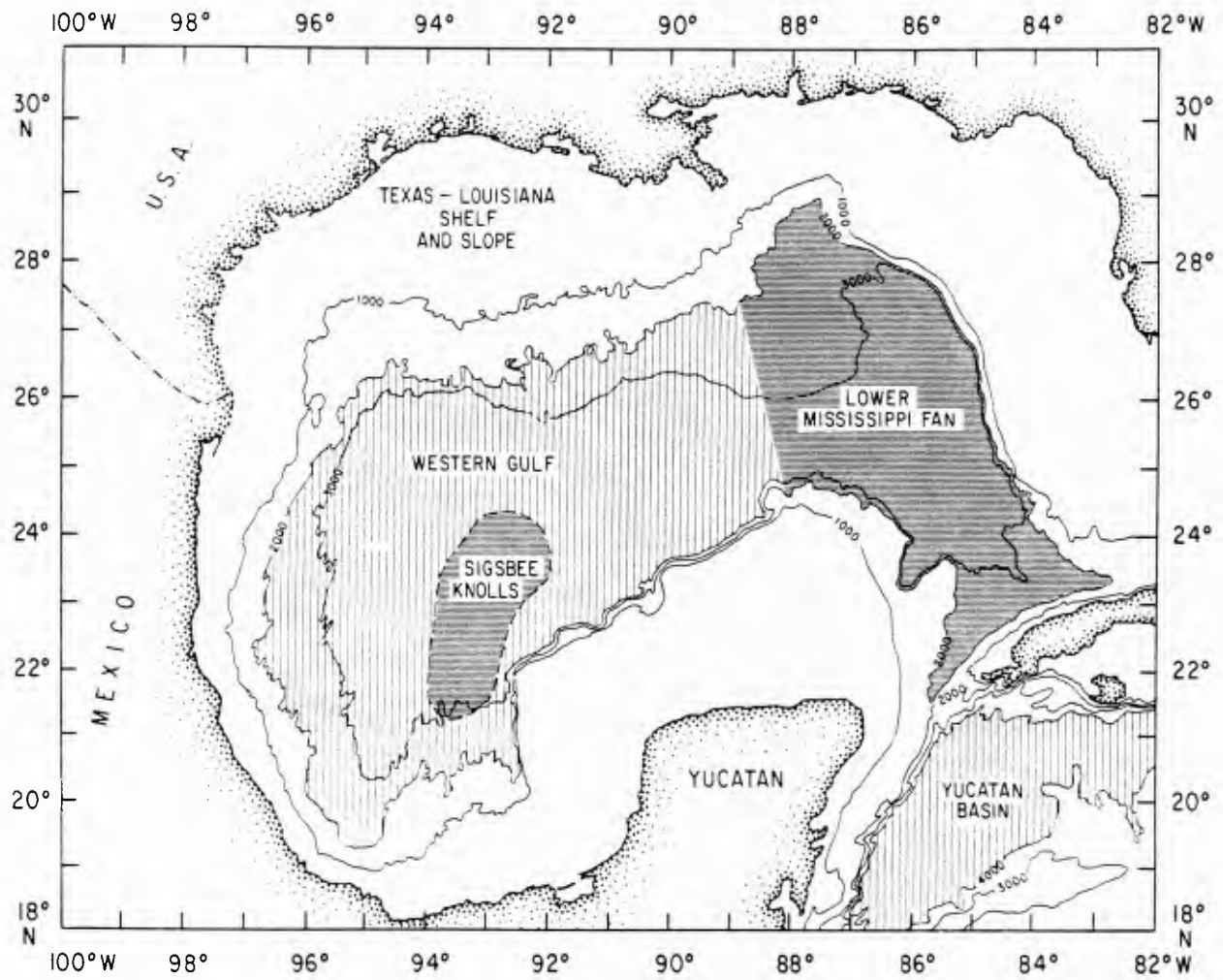
Reproduction in whole or in part is permitted
for any purpose of the United States Government.
Document cleared for public release and sale;
distribution unlimited.

ABSTRACT

Signal transmission loss and spatial coherence data for source-receiver separations between 100 and 250 km were acquired in the Gulf of Mexico with a calibrated seismic measurement system (400 m deep), a towed projector (100 m deep) which emitted 67 and 173 Hz tones, and a moored Webb sound source at 988 m depth driven at 175 Hz. Environmental data such as the range dependent bathymetry and sound velocity profiles were measured. The 67 Hz data showed a persistent sound transmission loss of approximately 90 dB whereas the 173 Hz showed several pronounced loss minima between 100-90 dB. Slope enhancements were found to be on the order 2-4 dB @ 67 Hz and 6 dB @ 173 Hz when compared to flat bottom calculations. Pair-wise coherence data show the combined effects of multipath interference and signal-to-noise ratio. Estimates of signal coherence length from the coherent summation of streamer hydrophones yield coherence lengths between 70 and 300 meters at a frequency of 173 Hz. Fast asymptotic coherent and normal mode transmission loss calculations produced results consistent with measured data for the deep flat portion of the measurement tracks when measured geo-acoustic profiles or related bottom loss curves were used. The implicit finite difference parabolic equation calculations were consistent with range-averaged data for the flat portion of the track as well as on the slope. These results show that if proper qualitative description of the sub-bottom velocity profiles are used, then computations with either a parabolic equation or normal mode technique are consistent with experimental results.

TABLE OF CONTENTS

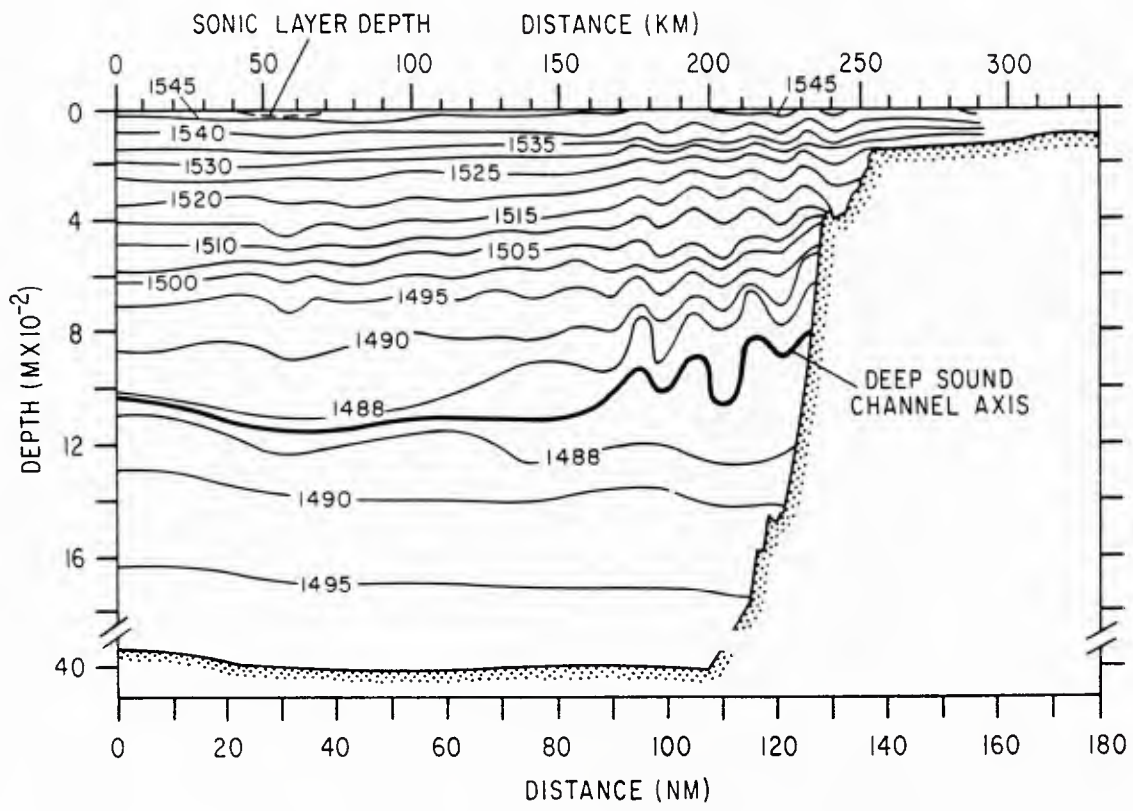
	Page
ABSTRACT.	i
THE PRESENTATION SLIDES	
1 - THE MAP OF THE GULF OF MEXICO	1
2 - SOUND VELOCITY PROFILES (SVP) VERSUS RANGE.	3
3 - ISOVELOCITY CONTOURS VERSUS RANGE	5
4 - A COMPOSITE OF THE SVP'S	7
5 - THE GEOACOUSTIC MODEL	9
6 - BOTTOM LOSS CURVES.	11
7 - MEASURED TRANSMISSION LOSS VERSUS RANGE	13
8 - A RAY-DEPTH-RANGE PLOT.	15
9 - ROOT-MEAN-SQUARE PRESSURE (dB re $1\mu\text{Pa}$), P_{rms} , VERSUS LENGTH	17
10 - MAGNITUDE-SQUARE COHERENCE, MSC, VERSUS LENGTH.	19
11 - FAST FOURIER TRANSFORM (FFT), COHERENT SUMMATION.	21
12 - A HISTOGRAM OF DIFFERENTIAL SIGNAL GAINS (DASG)	23
13 - A NORMAL MODE (SNAP) COMPARISON WITH DATA	25
14 - A NORMAL MODE (SNAP/ASTRAL) COMPARISON WITH DATA.	29
15 - HIGH ANGLE PARABOLIC CALCULATIONS COMPARED WITH DATA.	31
16 - HIGH ANGLE PARABOLIC CALCULATIONS COMPARED WITH OMNI-DATA	33
17 - SUMMARY OF RESULTS.	35
18 - CONCLUSIONS	37
REFERENCES.	40



SLIDE 1

This paper summarizes the results from an environmental acoustic experiment conducted in the Gulf of Mexico during 1979. B. Brunson was responsible for calculations performed with the oceanographic analysis of P. Bucca, geophysical data from J. Matthews and geoacoustic analysis of S. Mitchell. R. Wagstaff performed a series of noise directionality measurements in conjunction with this experiment; however those results will not be discussed in this paper.

The purpose of these experiments was to quantify the noise characteristics of a deep bottom limited basin. Central to this issue are the transmission characteristics presented and discussed in this paper. The specific case of down slope to bottom limited sound channel propagation is essential to determining the contribution of coastal sources to the mid-basin noise field. The ability to perform a reliable transmission loss calculation with either a geoacoustic model or a derived bottom loss curve provides a necessary basis for the calculation of mid-basin horizontal noise directionality. The determination of the signal coherence is also necessary for the computation of vertical noise directionality. The computer codes used to perform calculations for this paper were developed elsewhere. We simply use these codes to provide a quantitative tool in the interpretation of these data.

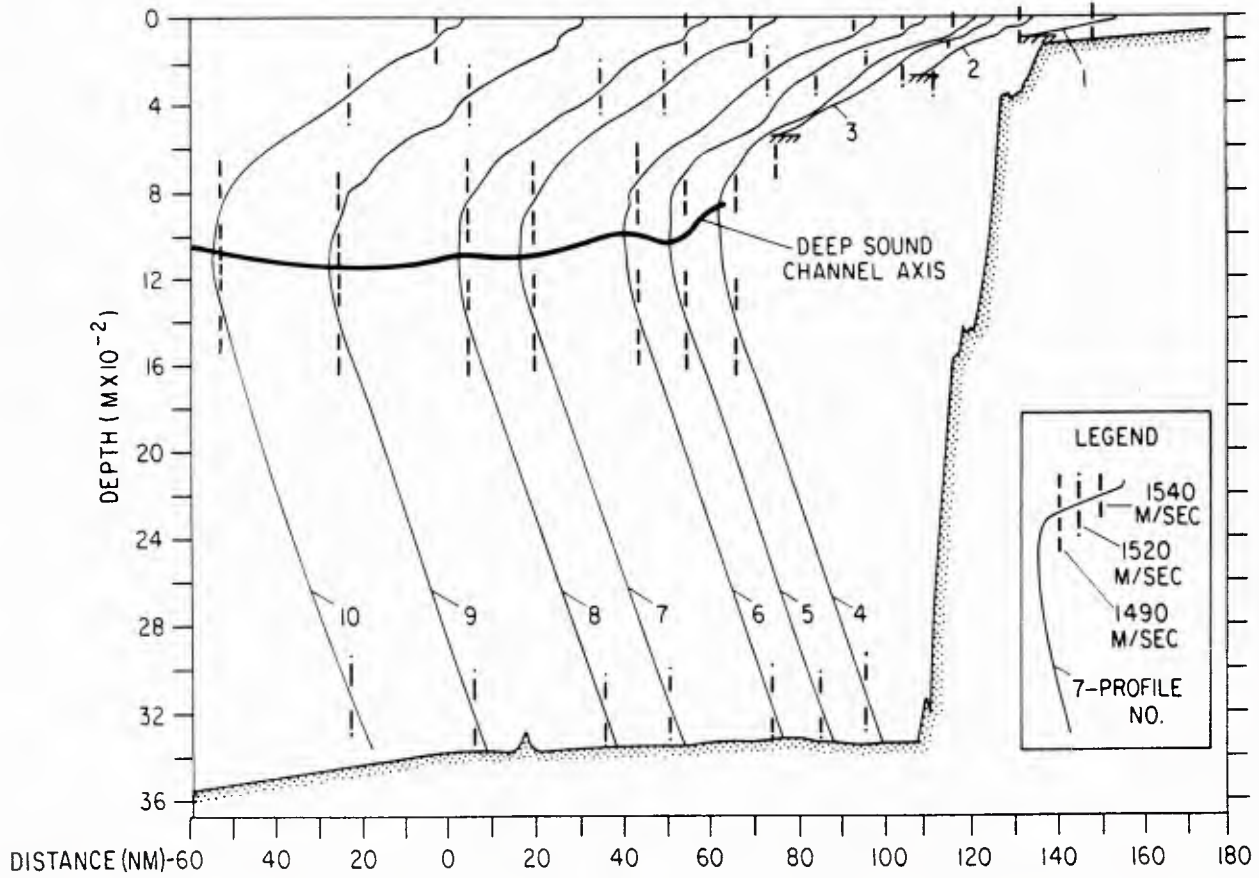


SLIDE 2

The track chosen for the down-slope propagation run was from the Florida Plain, the lower portion of the Mississippi Fan, toward the West Florida Escarpment. The bathymetry along the source track is shown from the receiver location. These isovelocity contours show the effect of the Loop Current (the variation in the deep sound channel axis) as one proceeds to the escarpment. The Yucatan Current enters the Gulf of Mexico with part proceeding east through the Straits of Florida and part proceeding west into the Gulf. This Loop Current and the anticyclonic gyres which separate from it constitute the major circulation feature of the Gulf of Mexico. The Northern penetration of the Loop Current is cyclic with periods on the order of 6 months to 1 year. At its Northern extreme the current turns east and then proceeds south to southeast until it joins the remainder of the current in the Straits of Florida. The isovelocity contours show the pronounced effect of this current at the deep sound channel axis with its influence still observed as one proceeds toward the surface. An issue addressed in this paper is the influence of this Current on the sound transmission.

DISTANCE (KM) — 100 50 0 50 100 150 200 250 300

PROFILE LOCATION — 10 9 8 7 6 5 43 2 1

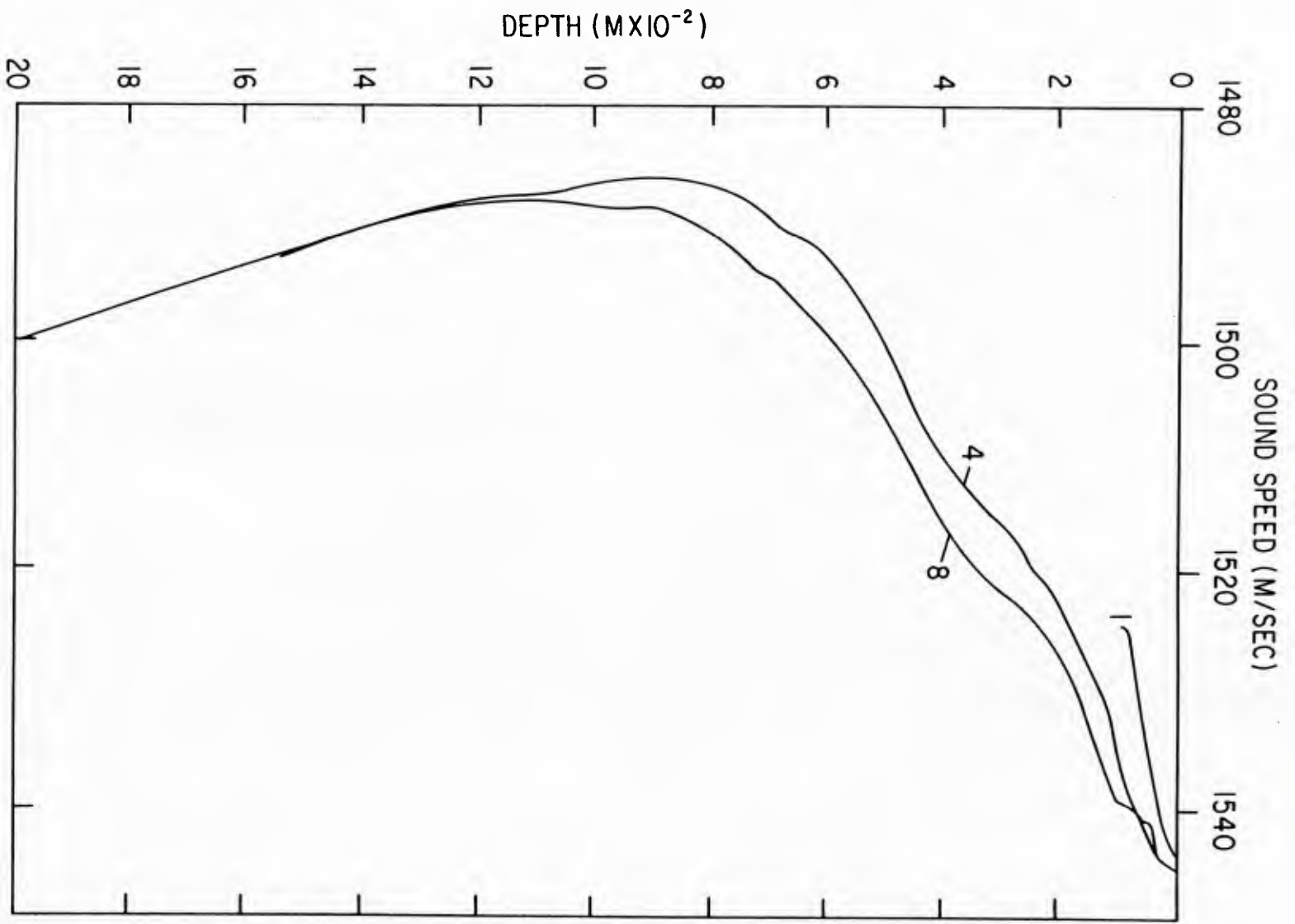


SLIDE 3

This slide shows ten representative measured sound velocity profiles corresponding to the previous isovelocity contours superimposed on the bathymetric profile. The bathymetry along the source track is essentially flat with an average depth of 3700 m. The West Florida Scarp is encountered at a range of 200 km from the receiver location and shoals to 385 m at 235 km with an average slope of 8.6° .

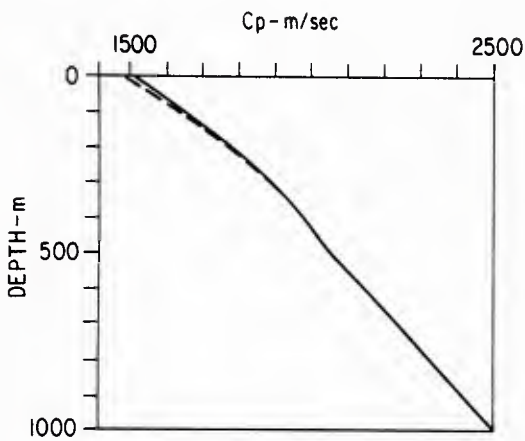
As stated earlier, the regional oceanography is affected by the Gulf Loop Current which manifests itself as a subsurface salinity maximum leading to a sound speed maximum between 100 and 200 m. The measured sound speed profiles indicate a sound speed maximum at 150 to 160 m leading to a weak channel centered about 110 to 130 m. A more significant feature of the sound speed field is that near surface sources are bottom limited over the entire track. The sound speed at 91 to 100 m is typically 1540 m/sec while the sound speed of the bottom (mid-track) is approximately 1525 m/sec. This yields a minimum grazing angle of 8° .

The bottom limited characteristic is representative of the Gulf of Mexico as a whole. As mentioned by Mitchell, the entire Gulf of Mexico is bottom limited with minimum grazing angles of 8° or greater.

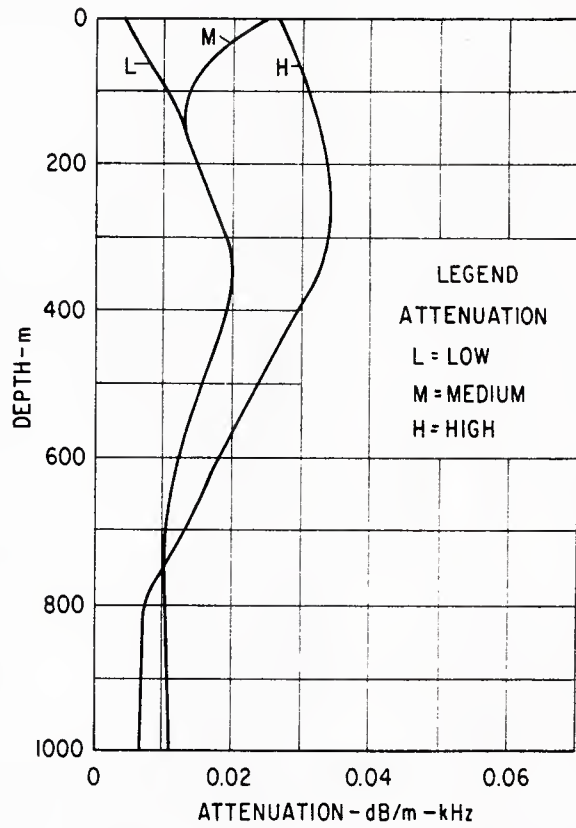


SLIDE 4

This slide shows a comparison of three profiles (1, 4, 8) shown on the previous slide over the track bathymetry. The steepening of the near surface gradient is observed as one proceeds from slope water (profile 1) to the deep portion of the track (profile 8). The formation of a near surface sound velocity maximum at approximately 160 m with a weak sound channel at approximately at 110 m is readily observed. The deep sound channel axis is also shown to increase in depth between profiles 4 and 8. All these characteristics are due to the presence of the loop current.



depth m	Lower Miss. Fan	Western Gulf
0-	1520 m/sec	1530 m/sec
0+	1482 m/sec	1504 m/sec
100	1636 m/sec	1652 m/sec
200	1770 m/sec	1780 m/sec
300	1885 m/sec	1888 m/sec
400	1979 m/sec	1976 m/sec
500	2052 m/sec	2044 m/sec
1000	2500 m/sec	2500 m/sec



SLIDE 5

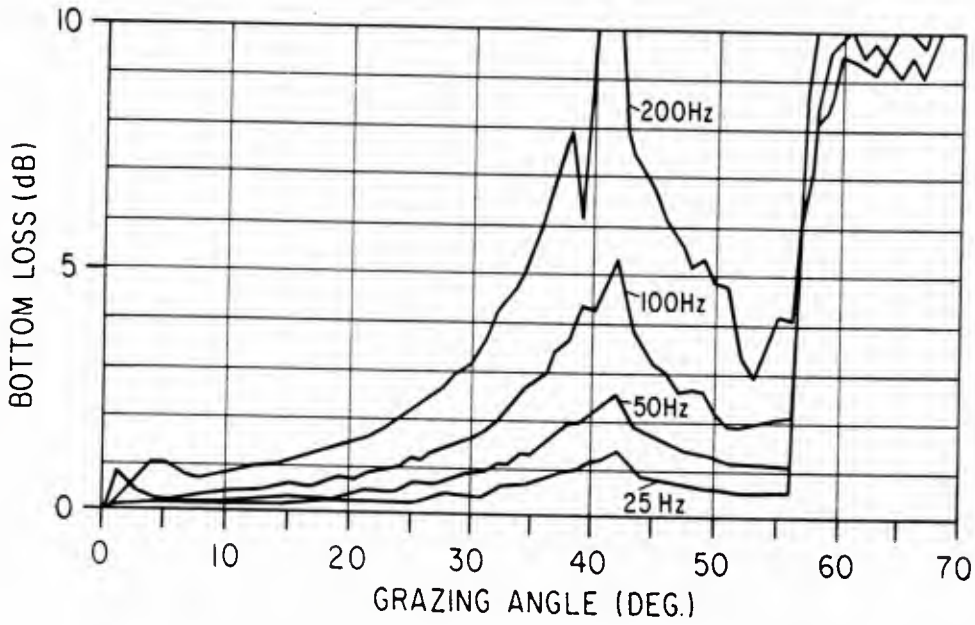
These geoacoustic profiles are based on the work of S. K. Mitchell, ARL/UT (1979) and J. Matthews, NORDA (1979). Since the Gulf of Mexico is bottom limited, the propagation of sound ($f < 200$ Hz) which interacts with the bottom will produce a specular component, the level of which depends on the density contrast, and a refracted component, the level of which depends on the frequency-depth dependent attenuation coefficient. The description of the refracted arrival can be described by the "geoacoustic" models of the ocean bottom discussed by Hamilton (1980).

The level of the refracted arrival is determined by the length of the refracted path and the attenuation coefficient. The refracted arrival could constitute much of the signal energy for frequencies less than 200 Hz and grazing angles less than 30° . Thus one requires the sediment sound velocity profile since it determines the refracted path length as well as the attenuation coefficient to describe the level of the refracted signal.

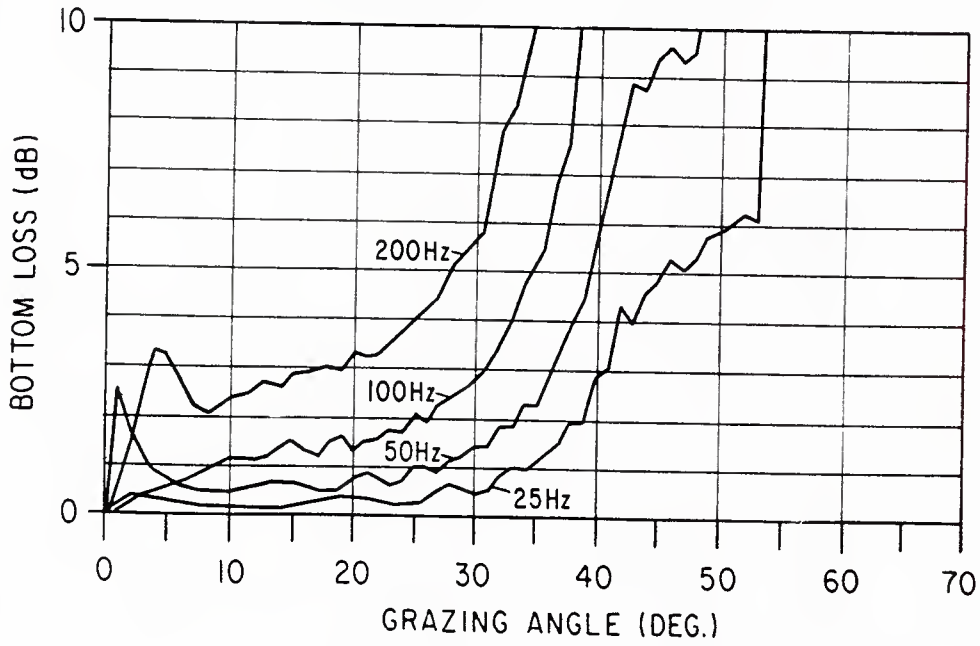
This slide shows the sound velocity profile versus depth for the eastern Gulf of Mexico region as determined by J. Matthews, NORDA, based on core samples and profiling records. Also shown are three estimates of the measured attenuation coefficients from similar sediments in the Indian Ocean. These curves represent a "geoacoustic model based on the available geophysical and geological survey data.

These geoacoustic parameters (sound speed, density, and attenuation) were used directly in calculations performed with parabolic equation and normal mode codes. These parameters were also used to derive bottom loss versus grazing angle curves as a function of frequency for calculations used with FACT and ray models.

LOW ATTENUATION



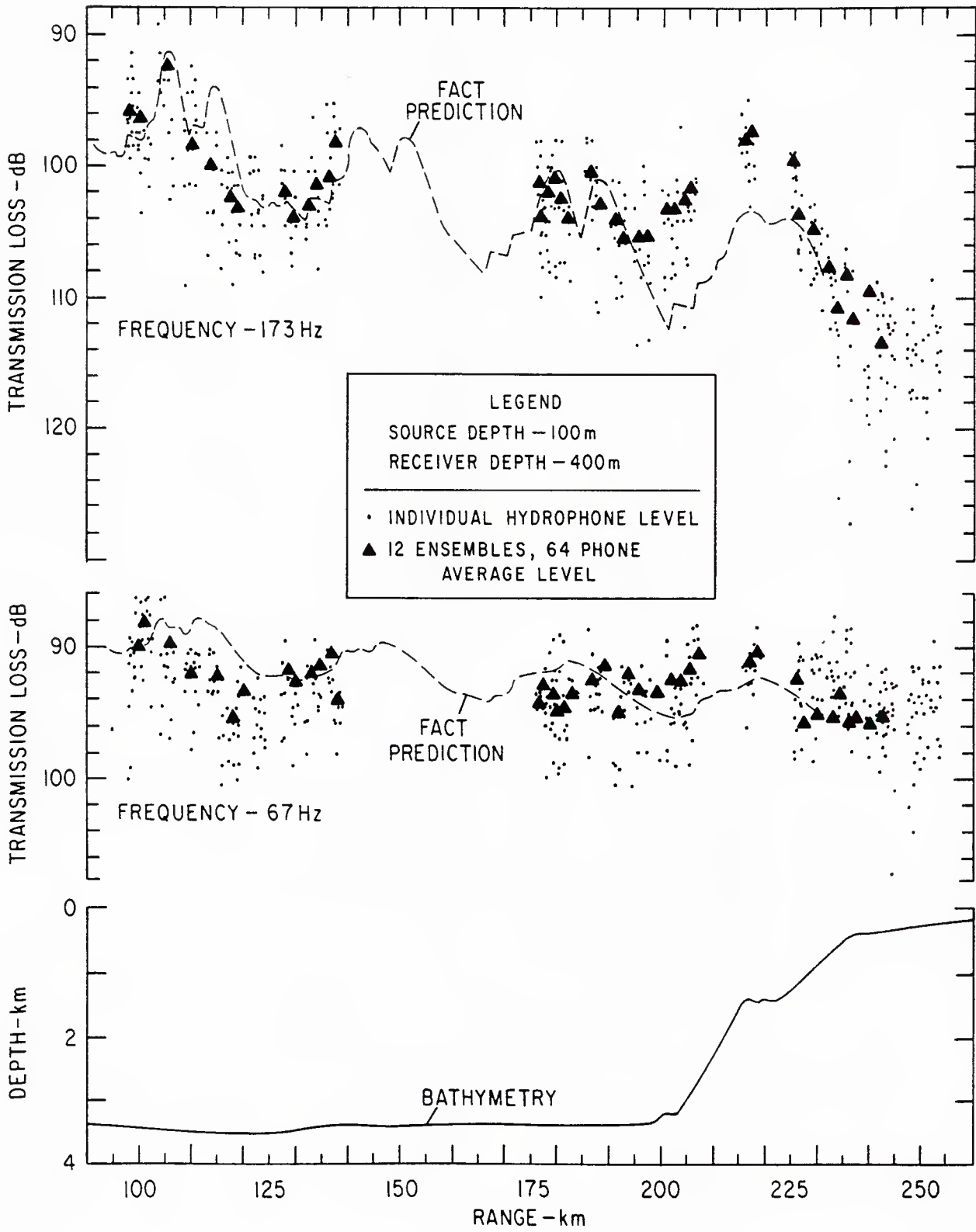
MEDIUM ATTENUATION



SLIDE 6

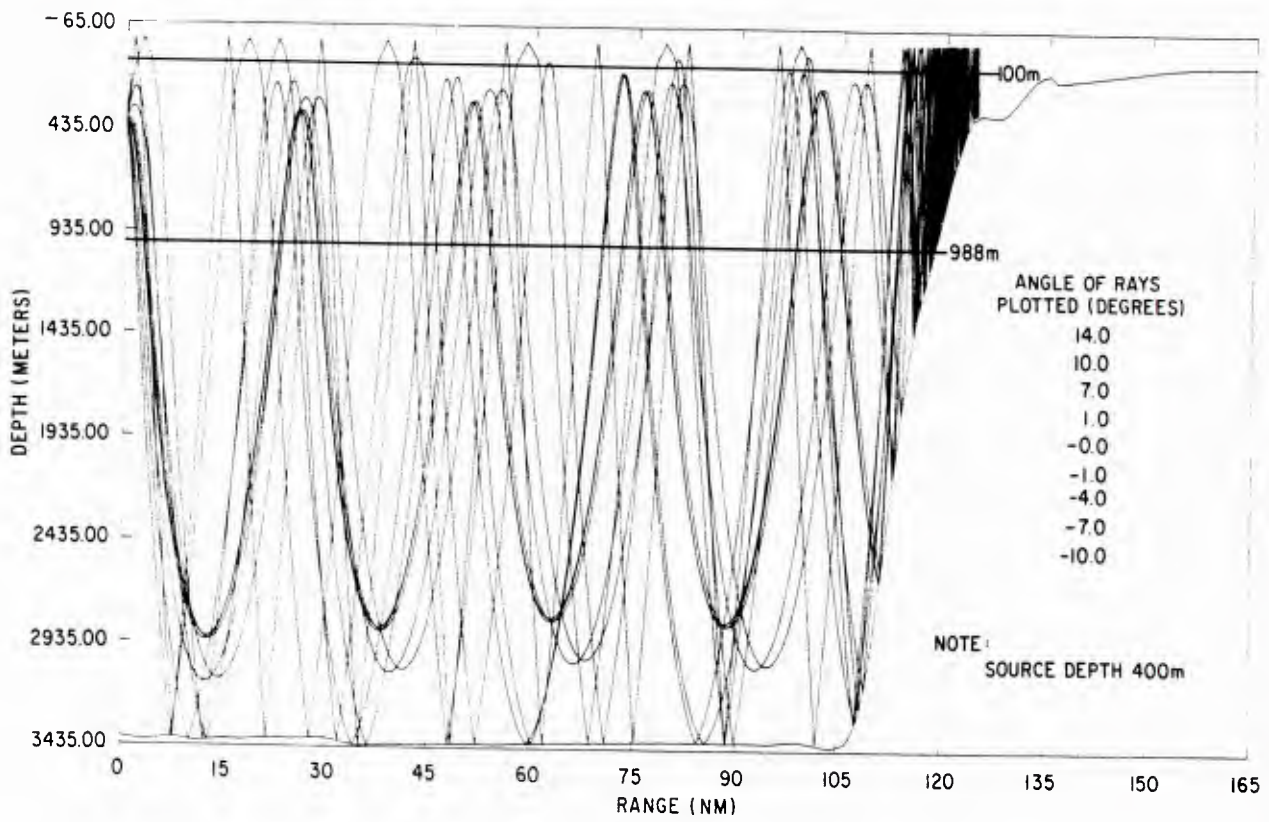
This slide shows bottom-loss curves derived by Mitchell (1979) from the previously shown compressional velocity and attenuation profiles. Bottom loss versus grazing angle are shown for the case of low and medium attenuation. In performing the calculation, Mitchell used a sediment thickness of 1000 m. The choice of sediment thickness was somewhat arbitrary, but since in this portion of the lower Mississippi Fan the sediment thickness is greater than several hundred meters, the effect of sediment thickness could only be important at grazing angles greater than 40° . These steep angles are not important along the deep portion of the sound transmission track. However, geoacoustic data and bottom loss estimates must be carefully used since the sediment thickness is changing, that is becoming shallower.

Empirical estimates of the bottom loss at an approximate angle of 10° were based on a ray trace model to determine the number of bottom bounces as a function of range and a 10 Log (R) rule. These estimates were found to be between 0-0.5 dB @ 67 Hz and 1.5-2.0 dB @ 173 Hz. As shown on this slide, the 173 Hz data is consistent with a medium attenuation curve while the 67 Hz data could be considered consistent with either the low or medium loss curves.



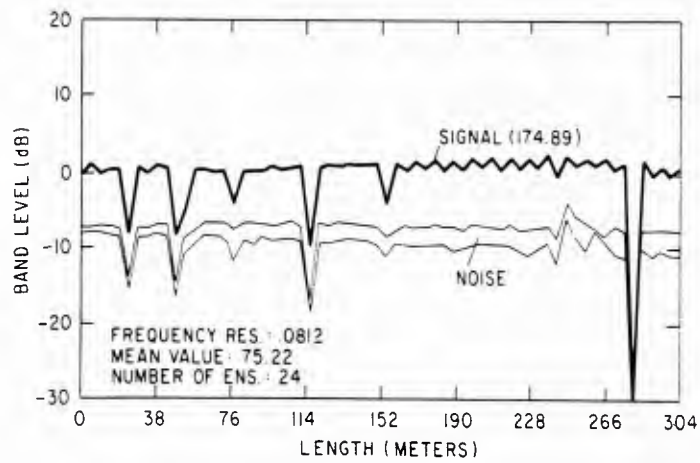
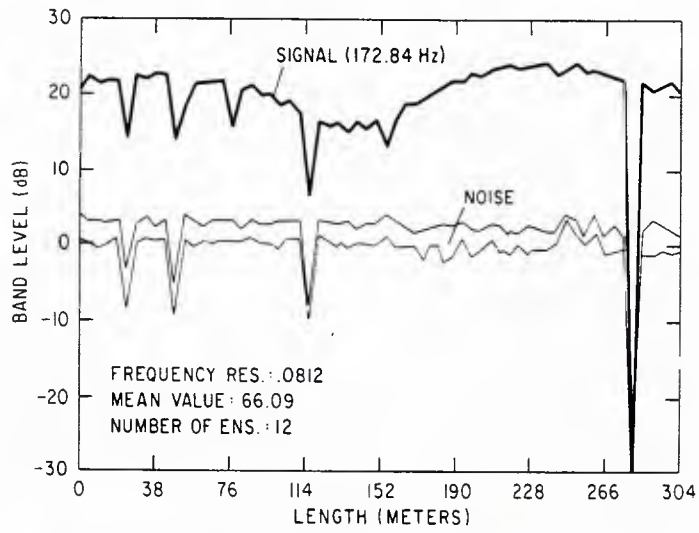
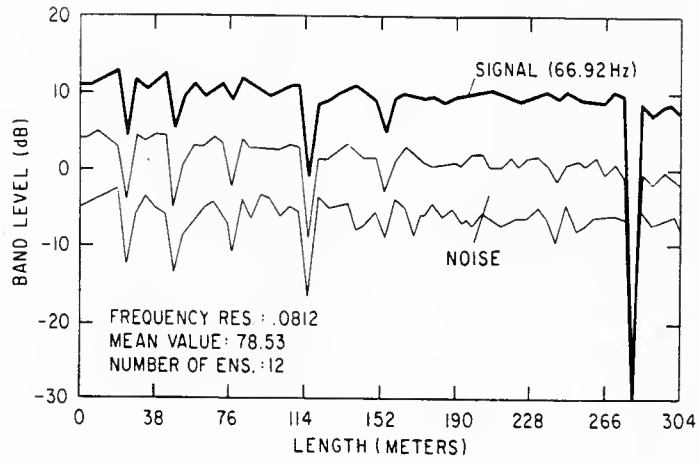
SLIDE 7

Transmission loss results are shown for 173 Hz (top), and 67 Hz (middle) on this slide. The triangular data points represent the transmission loss determined from the difference between the calibrated source level and range averaged received energy level. The range averaging was due to the source receiver motion for the individual hydrophone (the dots) and was between 1 and 2 km for the average of 12 (0.8 Hz, 12.5 sec) samples. The triangles represent the average response of 64 (minus dead hydrophones) phones over 304 m. The single hydrophone results show wider variation than the hydrophone-averaged results as one might expect. Also shown on this slide is the range dependent bathymetry (care must be taken to observe the change in scales). Based on empirical curve fits to these data a low attenuation bottom loss characteristic was chosen for the 67 Hz data and a medium for the 173 Hz data. These bottom loss curves were then used with Spofford's FACT Model to calculate transmission loss versus range at 67 and 173 Hz as shown. The agreement--on average--was found to be good. We observe that in this environment the 67 Hz transmission loss is 10 dB less on average than that at 173 Hz and much more uniform. We also observe the difference in slope enhancement taken as the difference between the data and the flat bottom FACT calculation. The 67 Hz data shows enhancements up to 6 dB with most points between 2 and 4 dB. The 173 Hz data shows peak enhancements of 6 dB but a drastic increase in TL as one proceeds up the slope. These data clearly show the improved transmission (at 67 Hz) at the lower frequency as well as the qualitative agreement with Spofford's FACT calculation.



SLIDE 8

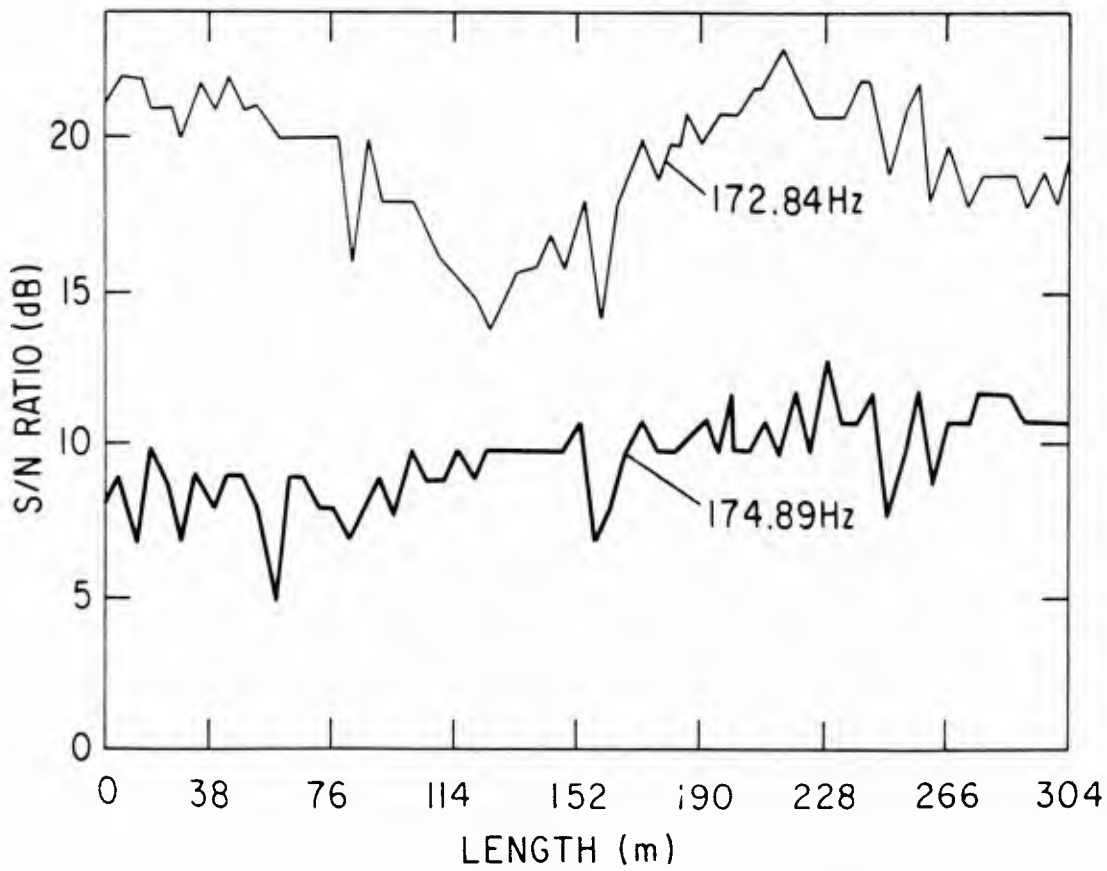
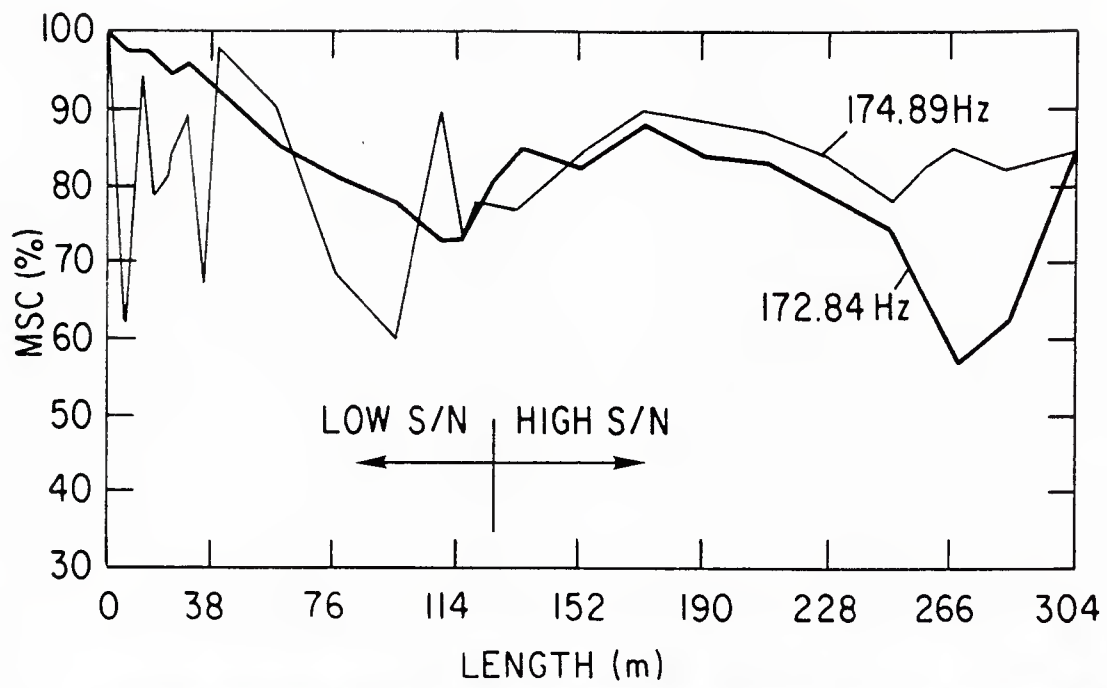
Here we show a range dependent ray trace corresponding to the profiles shown on Slide 3. This ray trace confirms our previous comments concerning the bottom limited characteristics of the transmission. The 100 m receiver, reciprocity being employed, only receives bottom limited energy in a narrow band near the limiting ray. The higher angle energy is drastically stripped from the 173 Hz signal yielding the minima and maxima on the transmission loss curve. The 67 Hz data suffers a good deal less loss (~10 dB) and represents a wider angular spread near the limiting ray and, consequently, we receive more energy along the track and a smoother transmission loss characteristic. The choice of the "low" or "medium" loss curves for the FACT model were based on an empirical estimate of the bottom loss per bounce near grazing angles of 10^0 between 0-0.5 dB at 67 Hz and 1.5-2 dB at 173 Hz.



SLIDE 9

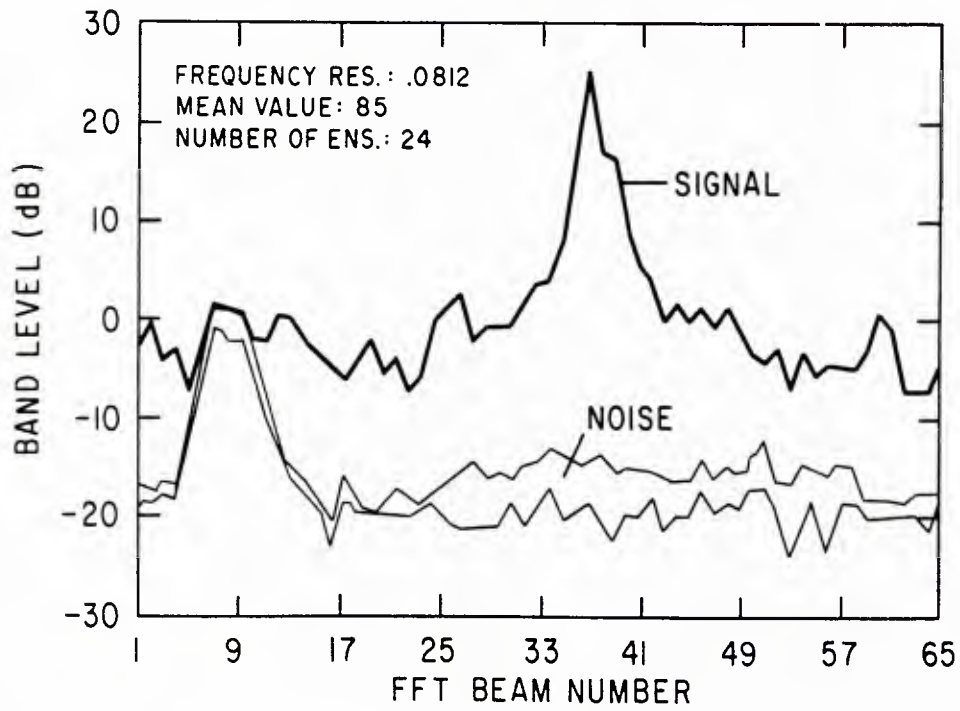
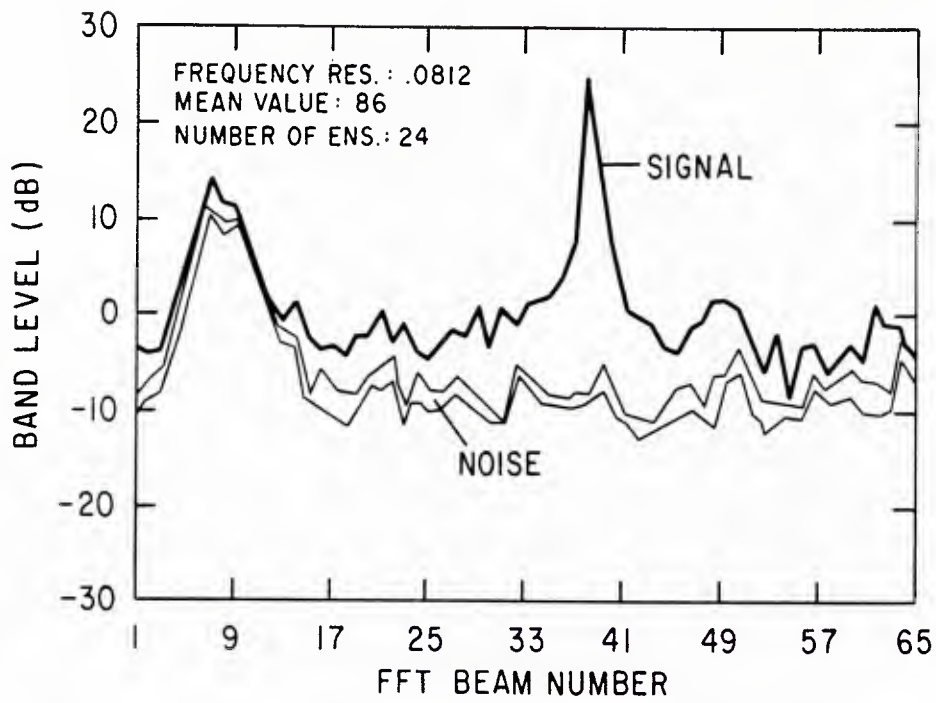
Before discussing the coherence of the signal I would like to show a few illumination functions, Prms (root-mean-square pressure) versus length. This slide shows the root-mean-square pressure in dB versus the transverse aperture length for both signal and noise. The sharp dropouts represent hydrophones which were either dead or possessed low gain and were not used. The top figure shows the results for the 67 Hz tone which is a uniform distribution in pressure across the array. The two noise curves show the band of rms noise level spaced in frequency up and down from the signal frequency bin.

The second part of this slide shows the 173 Hz tone and an interference pattern due to the coherent addition of multipaths arriving off broad side to the array. The third portion of the figure shows the 175 Hz tone from the moored, 988 m, Webb sound source. The rapid undulations in the signal and noise curve are consistent with the beat of a near broadside arrival of up and down coming rays and a slight droop in the array as one proceeds towards the end of the array.



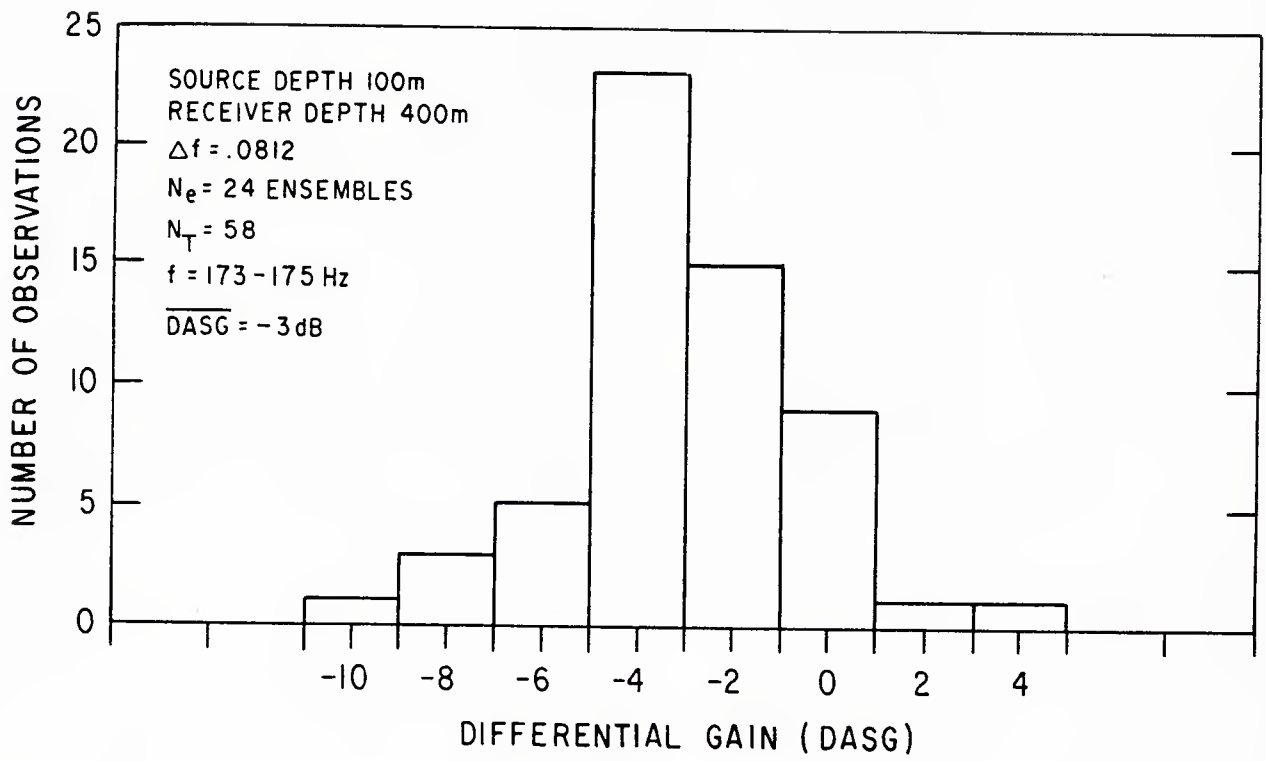
SLIDE 10

During the same interval of time we computed, from the data, the signal-to-noise ratio and magnitude square coherence (MSC) versus aperture length. The 173 Hz tone shows the previously mentioned multipath interference pattern which is also reflected in the MSC portion of the figure (top). The 175 Hz tone shows gradual increase of S/N as one proceeds down the array (Tow ship radiated noise (TSRN)). This is consistent with the decrease in coherent tow ship radiated noise. The coherent noise results in a rapid variation of the MSC (top) near the ship. As the S/N increases due to the decrease in TSRN this interference is reduced. This slide illustrates the difficulty in estimating coherence lengths from MSC versus length. The MSC replicates the multipath interference pattern and is sensitive to the noise characteristics. I refer the interested experimentalist to the work of Carter at NUSC for a detailed treatment of the estimation of coherence of a signal imbedded in a random noise background.



SLIDE 11

Another measure of the coherence is the coherent gain of the system. This slide shows the time averaged coherent output of the hydrophone groups. At the top one clearly sees the separation of signal energy and towship noise. At the bottom one clearly sees the response of the high signal level 173 Hz tone. The estimation of received coherent signal energy is easily performed at these signal-to-noise ratios. In these instances the averaging was such that too long a time was used when one considers the source receiver motion. Nevertheless, the peak signal-levels provide a good measured coherence if the mean hydrophone level is known and a functional form of the coherence versus transverse distance can be hypothesized. That is to say the difference between $20 \text{ Log } (N)$ and the measure gain, referred to here as DASG, is a measure of the degree in signal randomness or degree of coherence. The measurement uncertainties are reduced due to the high beam signal-to-noise ratios and the increased number of degrees of freedom.



SLIDE 12

This slide shows the result of the differential array signal gain analysis (DASG). The coherent summation of hydrophone group outputs corresponds to phase corrected addition of complex Fast Fourier Transform (FFT) coefficients. The differential array signal gain (DASG) was taken to be 10 Log the ratio of the peak beam signal power and the mean hydrophone signal power divided by the number of the elements squared (N^2). The DASG corresponds to 10 Log the summation of the pairwise coherence estimates normalized by N^2 .

$$DASG = 10 \cdot \text{LOG}_e(\langle S_B \rangle / \langle S_H \rangle / N^2) = 10 \text{LOG}_e \left\{ \sum_x \sum_j \rho_{xj} / N^2 \right\}$$

Thus if we have a knowledge of the coherence function

$$\rho_{xj} = \text{EXP}((\Delta_{ij} / L_c)^m)$$

where Δ_{ij} is the separation between the elements and L_c is a coherence length; then given a measure of DASG we can estimate L_c . A natural choice would be to assume either a Gaussian or an exponential functional form for the coherence function such as Cox employed in his 1973 JASA article. This exponential function is interesting as a closed form expression for array signal gain is realized. However, an exponential coherence function implies a discontinuous physical process which may not be applicable to acoustic waves weakly scattered by the ocean surfaces and volume.

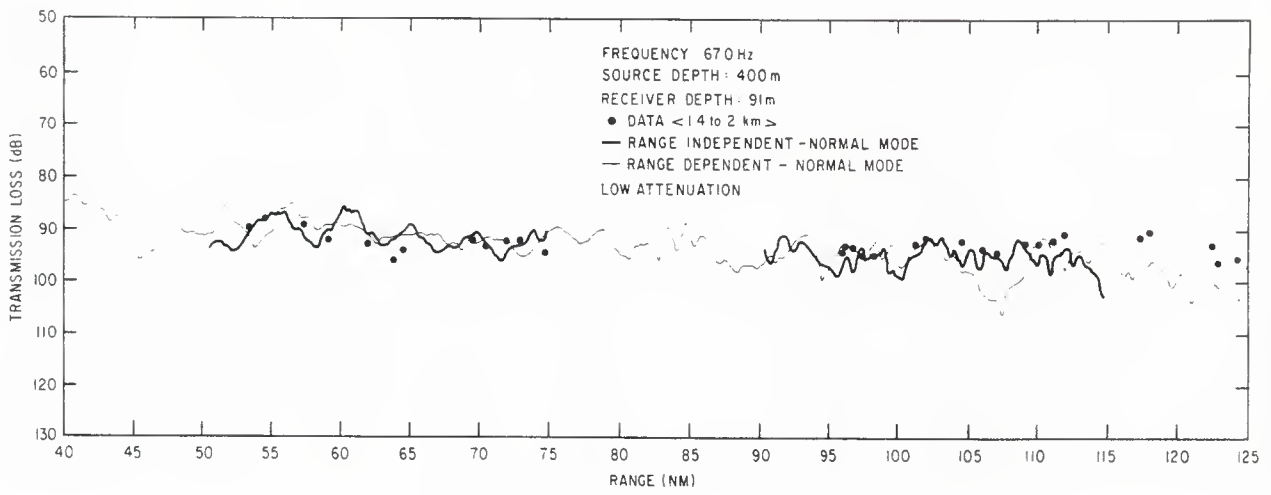
In the case of volume scattering, Beran and McCoy have employed an expression with $n = 1.5$ whereas Flatte and Dashen use $n = 2$, the Gaussian form. While these papers discuss volume scattering from internal waves and may not be applicable to surface scattering or bottom interacting problems, it is interesting to note that if we can model the bottom limited transmission as a two liquid layer, then the volume inhomogeneities in the sediment may produce coherence functional forms similar to those observed above. Brekhovskikh has also shown that the surface scattering coherence function depends on the square of the coherence parameter and has in some cases a Gaussian form.

Shrifrin (1971) references Chernov (1960) and Tatarski (1961) and suggests that in general a Gaussian coherence function is adequate for most statistical antenna problems.

We simply employ for our purposes coherence functions with $n = 1.5$ and 2.0 to bracket the coherence lengths observed in this experiment.

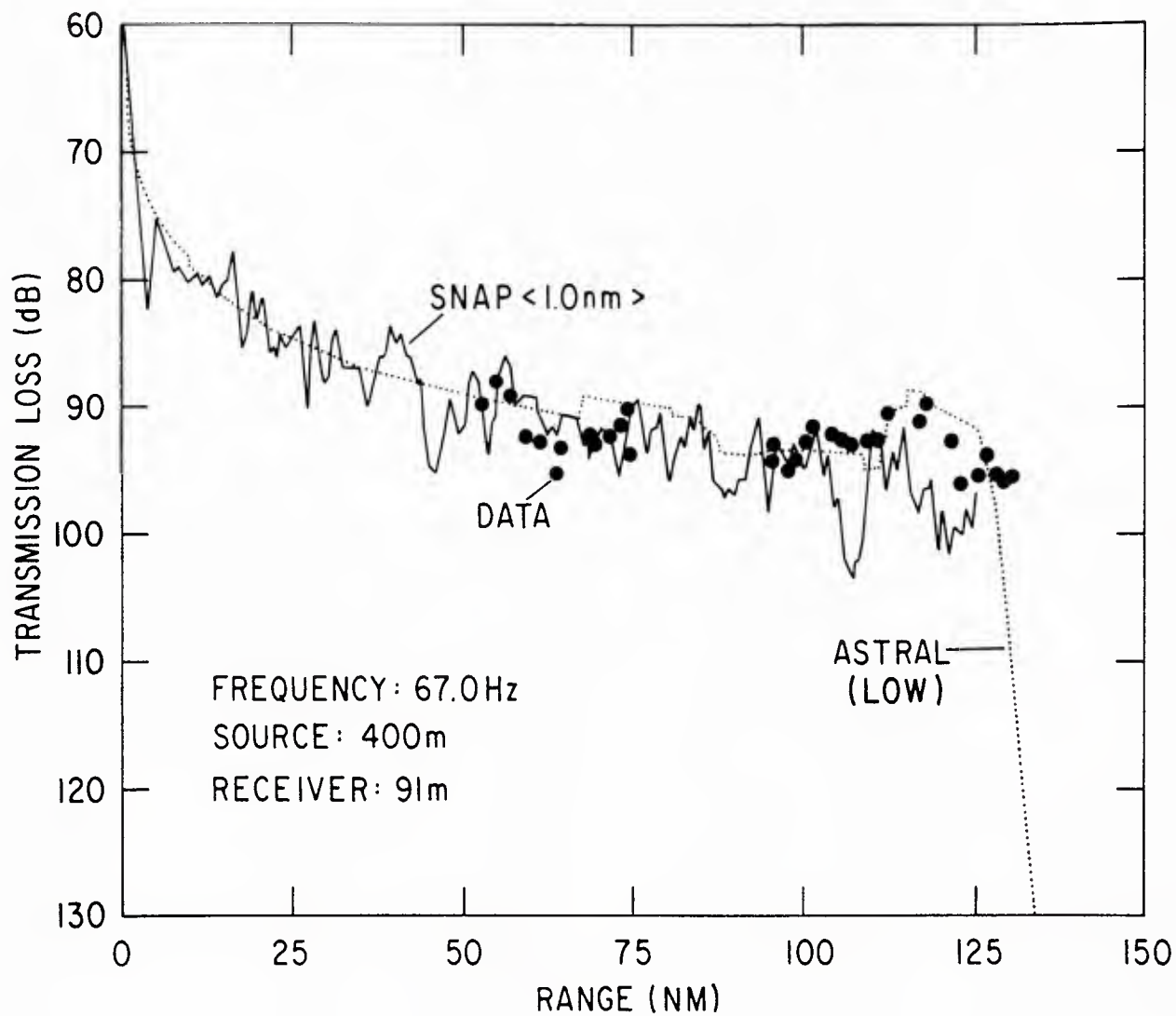
The histogram of DASG has a mean of -3 dB below the theoretical value of $20 \log(N)$. Also note some values of DASG are positive and these points result from our underestimation of the mean hydrophone signal power. This would correspond to an estimate of a coherence length of approximately 100 m (based on $n = 1.5$ or 2). Since the processing time was 17 minutes and since no peak tracking was employed, we estimate that at least 1.5 dB of the degradation could be due to source receiver motion. This would place our estimate of coherence length at 181 m ($n = 2$) and 200 m ($n = 1.5$). In several instances ideal gain was measured indicating coherence lengths greater than 304 m.

Thus employing the Gaussian form we bound the coherence length of the signal. In this instance our estimates range between 70 and 300 m with a mean value on the order of 180 m or greater. In summary the signal has retained some of its coherence at 173 Hz and we suspect that greater coherence lengths apply at 67 Hz.



SLIDE 13

We now turn to the issue of predictability given adequate environmental information concerning the water column and bottom. The normal mode computer code developed at the SACLANT ASW Research Centre was used to perform calculations for the deep basin portion of the track. This slide shows a comparison between range averaged data, a range independent calculation, and an adiabatically range dependent calculation using the range dependent sound velocity profiles and bathymetry. The agreement between all three is encouraging and leads to the conclusion that the loop current does not have a major influence on the transmission loss for this source receiver combination. Comparisons between calculations and data reveal that at 67 Hz the low attenuation bottom loss model provided the best fit. Thus at 67 Hz the low attenuation bottom seems appropriate for the lower Mississippi Fan. This result is consistent with the semi-empirical estimates and FACT results discussed earlier.

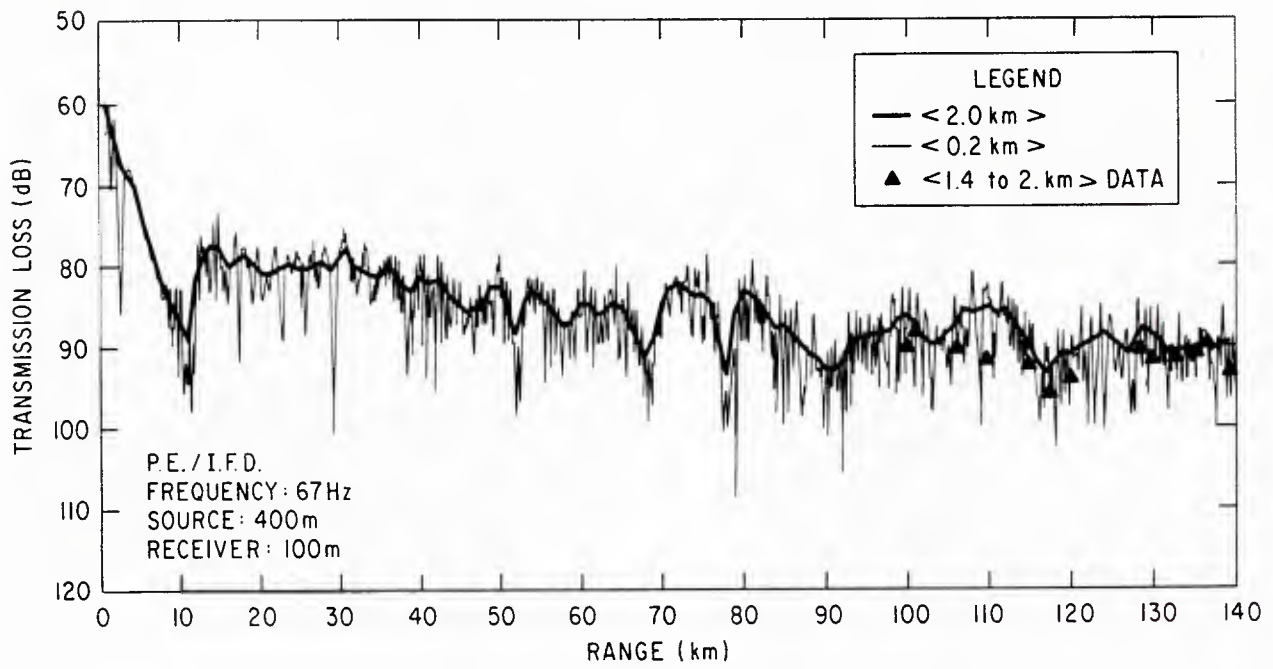


SLIDE 14

Several calculations were made using the measured bathymetry, sound speed, and the previously discussed geoacoustic model of the bottom. This slide shows results indicative of the calculations performed with a normal mode computation which assume the process is adiabatic (SNAP) and a normal mode computation which although adiabatic is a range smoothing transmission loss calculation (ASTRAL). The SNAP calculation employed the geoacoustic model directly, whereas the ASTRAL calculation used the derived bottom loss curves. The range-averaged data and the calculations were found to agree on average. The SNAP calculation was a flat bottom calculation and was not used to predict the slope enhancement.

The Astral calculation was performed over the slope. The mean level of slope enhancement is indeed predicted by this calculation; however, the fine structure in the transmission loss data shown previously was not predicted, as one might expect from a range averaged calculation.

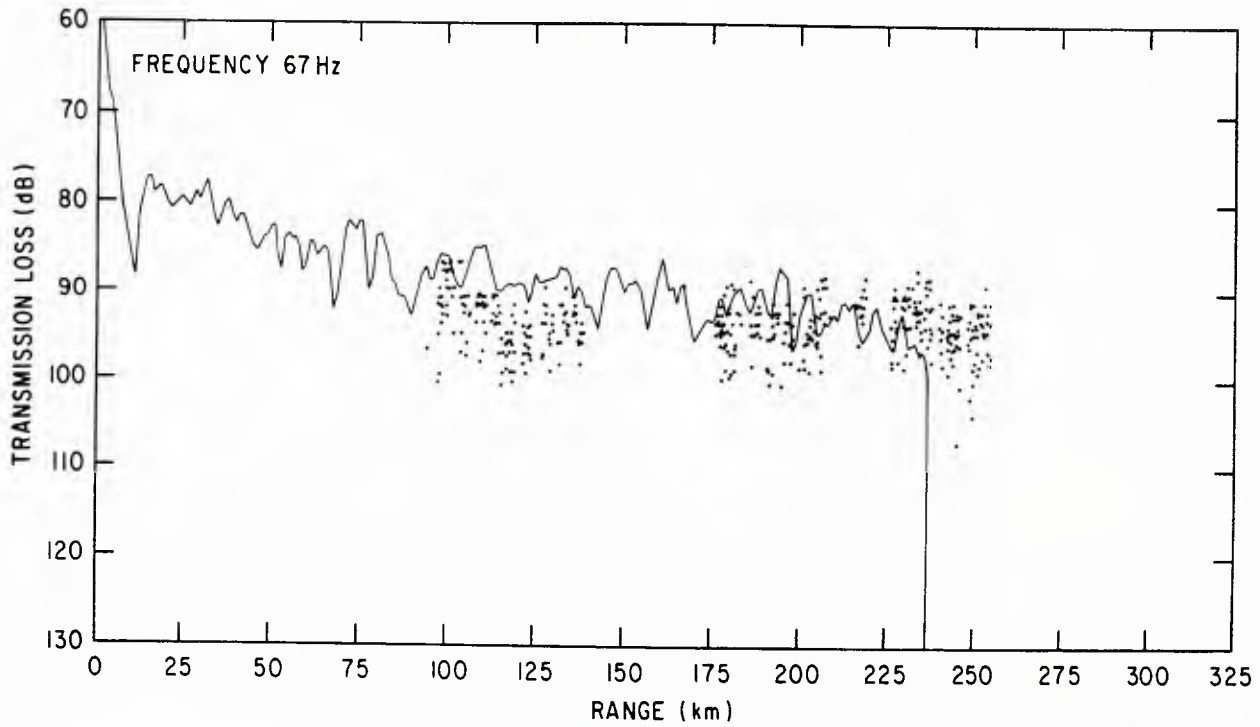
The calculated values are consistent with the data over the slope and indicate slope enhancements of up to 6 dB compared to the flat bottom calculations. These slope enhancements were larger than those estimates from the flat bottom FACT calculations which were found on average up to 4 dB at 67 Hz. This agreement in level between the data and calculations indicates the choice of the medium bottom loss curve and geoacoustic model was adequate.



SLIDE 15

The high angle parabolic equation code used to perform these calculations is described by Lee and Botseas (1982, 1983). This code uses an implicit finite-difference (IFD) scheme to solve the parabolic wave equation and can accommodate propagation angle of 40° measured from the horizontal. The range dependent model requires the bottom's compressional velocity, compressional attenuation and density as a function of depth.

Here we show a comparison of calculations averaged over 0.2 and 2 km with the range averaged transmission loss data. The calculations predict on average less transmission loss than measured. Nevertheless the agreement is considered adequate. The 0.2 km average data exhibits a spread around the mean with pronounced minima and maxima similar to the omnidirectional hydrophone data shown earlier.



SLIDE 16

These individual hydrophone levels are shown on this slide to compare favorably with the data for averaging of 2 km. Between 100 and 150 km we see that minima in the calculated transmission loss and data are comparable. However, on average the calculation underestimates the loss. Between 175 and 230 km we see good agreement before we reach the slope and then an over-estimation of the loss over the slope. The results of the calculations are stopped at a range of 230 km. These calculations show we are close with the geoacoustic model used in this calculation. However, the attenuation and sediment thickness on the slope may be incorrect.

SUMMARY

● SOUND TRANSMISSION RESULTS

f	TL (dB)	S.E. (dB)	BL@10 ⁰	LC
67 Hz	94	2-4	0-0.5	--
173 Hz	104	6	1.5-2.0	RANGE 70 TO 300 m MEAN 180 TO 200 m

● AGREEMENT WAS FOUND BETWEEN DATA AND CALCULATIONS

MODEL	f(Hz)	BL	<ΔR>	
SNAP	67	LOW	1.4-2 km	RANGE & RANGE INDEPENDENT
FACT	67	LOW	.9 km	RANGE INDEPENDENT
	173	MED	.9 km	
SSPE	67	C.A. = 15 ⁰	2 km	RANGE DEPENDENT
	173	C.A. = 10 ⁰	2 km	RANGE DEPENDENT
HAPE	67	GEO		

● DIFFICULTIES WITH SLOPE EXCEPT FOR ASTRAL

SLIDE 17

The results of this paper are summarized on this slide. The transmission of sound down-slope and in this bottom limited region was characterized by a loss of 94 dB @ 67 Hz compared to 104 dB @ 173 Hz. The received signal characteristics at 67 Hz were more uniform than at 173 Hz, reflecting the importance of the bottom refracted energy at 67 Hz. This result is consistent with the estimated bottom loss at 10^0 grazing angle to be 0-0.5 dB @ 67 Hz and 1.5-2.0 dB @ 173 Hz. While the loss is greater at 173 Hz, the slope enhancement at the beginning of the slope was found to be more pronounced than that of 67 Hz, but the loss increased markedly as one proceeds up the slope compared to the persistence observed in the 67 Hz data. Estimates of mean coherence lengths at 173 Hz were found to be 180 m based on a Gaussian coherence functional form representing, in the opinion of the authors, a lower bound.

The results presented here were shown to agree on an average level basis with a wide variety of computations. This agreement resulted from the use of measured environmental factors such as bathymetry, sound velocity profiles and geophysical data. Although no detailed comparison was presented the calculations performed with the geoacoustic model or derived bottom loss curves were found to have a spread between the minima and the maxima comparable to the data. Difficulties were encountered with calculations over the slope; however, ASTRAL appeared to perform very well on the average.

The differences observed at 67 Hz between data and FACT model slope enhancements of up to 4 dB compared to calculated enhancements of up to 6 dB may indicate that the extension of the geophysical data and consequently the geoacoustic model to the slope may not be justified. This extension may provide for the propagation of high angle energy thus overestimating slope enhancement.

CONCLUSIONS

WE CONCLUDE THAT:

- O GIVEN THE GEOACOUSTICS - FAIR AGREEMENT
- O PROPAGATION (LF 67 HZ) INSENSITIVE TO LOOP CURRENT
- O BASIN RANGE INDEPENDENT MODELS ARE ADEQUATE
- O OBSERVED SLOPE ENHANCEMENTS GREATER THAN PREDICTED MEANS SLOPE-GEOACOUSTICS IS AN UNRESOLVED ISSUE
- O SIGNAL COHERENCE ON THE ORDER OF 20-23 WAVE LENGTHS CAN BE OBSERVED WHEN SEDIMENTS ARE THICK

SLIDE 18

We conclude, based on the calculations and experimental data presented in this paper, that given the correct geoacoustic description of the bottom and adequate description of the water column properties, that calculations performed with a wide variety of computer models yields fair agreement with the experimental data. Since all the calculations employed in this paper neglect shear, we conclude that in this frequency range 67-173 Hz and for water depths on the order of 100 m or greater and sediment depths sufficient therefore conclude that with judicious selection of the sound velocity profile noise characteristics for sources in the basin can be described using range independent models. It must be stressed that this result is a consequence of the near surface velocity profile, which makes this whole region bottom limited. Thus, the transmission characteristic is primarily due to the influence of the bottom. This conclusion drastically simplifies our problem in estimating mid-basin ambient noise directionality.

For the source-receiver geometries employed in this experiment the qualitative aspects of the transmission characteristics were adequately described by range independent models compared to the range dependent calculation. We therefore conclude that with judicious selection of the sound velocity profile noise characteristics for sources in the basin can be described using range independent models. It must be stressed that this result is a consequence of the near surface velocity profile which makes this whole region bottom limited. Thus the transmission characteristic is primarily due to the influence of the bottom. This conclusion drastically simplifies our problem in estimating mid basin ambient noise directionality.

A significant result from this experiment is the estimation of the coherence length of the 173 Hz signal of 200 m. Since we attribute a decrease in coherence due to a randomness introduced as a result of scattering this result implies that at lower frequencies, longer wavelengths, the coherence lengths are greater, that is until the rough surface of the basalt is reached. We therefore conclude that for signals refracted in this type of sedimentation that average coherence lengths greater than 180 m are possible. We recognize that scattering from a rough basalt-sediment interface would result in a different effect. Nevertheless for those regions

where sediment thickness and compressional wave velocity gradients are such that energy with grazing angles less than 30° is refracted, we conclude the energy will be coherent at least to lengths greater than 20-23 wavelengths.

REFERENCES

1. Mitchell, S.K. "Pre-Exercise Estimates of Bottom Interaction in the Gulf of Mexico and the Caribbean Sea," ARL/University of Texas, Austin, Texas, January 1979.
2. Matthews, J., Private Communication, Naval Ocean Research and Development Activity, Bay St. Louis, Mississippi, January 1979.
3. Bucca, P., Private Communication, Naval Ocean Research and Development Activity, 1979.
4. Hamilton, E.L., "Geoacoustic Modeling of the Sea Floor," J. Acoust. Soc. Am. 68(5), 1313-1340, (1980).
5. Spofford, C.W., "The FACT Model," Maury Center for Ocean Science, MC Report 109, Washington, DC, November 1974.
6. Spofford, C.W., "The ASTRAL Model Vol. 5," SAI-79-742WA, SAI, Inc., Westpark Drive, McLean, Virginia, January 1979.
7. Carter, C.G. and Scannell, E.H., "Confidence Bounds for Magnitude-Squared Coherence Estimates," NUSC TD 5881, Naval Underwater Systems Center, New London, Connecticut, 13 July 1978.
8. Cox, H., "Line Array Performance when the Signal Coherence is Spatially Dependent," J. Acoust. Soc. Am. 54, 1743-1746 (1973).
9. Beran, M.J., McCoy, J.J., "Directional Spectral Spreading in Randomly Inhomogeneous Media," J. Acoust. Soc. Am. 66, 1468-1471 (1979).
10. Flatte, S.M., Dashen, R., Munk, W., Zachariahsen, "Limits on Coherent Processing due to Internal Waves," Stanford Research Institute, TR JSR 76-14, June 1977.

11. Brekhovskikh, L., Lysanov, Yu., "Fundamentals of Ocean Acoustics", Springer-Verlag, New York, 1982.
12. Shifrin, Y.S., "Statistical Antenna Theory," The Golem Press, Boulder, Colorado, 1971.
13. Chernov, L.A. "Wave Propagation in a Random Medium," McGraw Hill, New York, 1960.
14. Tatarki, V.I., "Wave Propagation in a Turbulent Medium," McGraw Hill, New York, 1961.
15. Jensen, F.B., and Ferla, M.C., "SNAP: The SACLANT Normal Mode Acoustic Propagation Mode," SACLANT Memorandum SM-121, 15 January 1979.
16. Lee, D. and Botseas, G. "IFD: An Implicit Finite Difference Computer Model for Solving the Parabolic Equation," Naval Underwater Systems Center, TR 6659, 27 May 1982.
17. Lee, D. and Botseas, G., "IFD: Wide Angle Capability," Naval Underwater Systems Center, TR 6905, 28 October 1983.

U221260